nature neuroscience

RNAi reveals doublecortin is required for radial migration in rat neocortex

Jilin Bai, Raddy L Ramos, James B Ackman, Ankur M Thomas, Richard V Lee & Joseph J LoTurco

Mutations in the doublecortin gene (*DCX*) in humans cause malformation of the cerebral neocortex. Paradoxically, genetic deletion of *Dcx* in mice does not cause neocortical malformation. We used electroporation of plasmids encoding short hairpin RNA to create interference (RNAi) of DCX protein *in utero*, and we show that DCX is required for radial migration in developing rat neocortex. RNAi of DCX causes both cell-autonomous and non-cell autonomous disruptions in radial migration, and creates two disruptions in neocortical development. First, many neurons prematurely stop migrating to form subcortical band heterotopias within the intermediate zone and then white matter. Second, many neurons migrate into inappropriate neocortical lamina within normotopic cortex. *In utero* RNAi can therefore be effectively used to study the specific cellular roles of DCX in neocortical development and to produce an animal model of double cortex syndrome.

Newly generated neocortical neurons migrate in a precise temporal pattern to form the layers of cerebral neocortex. The earliest-generated neurons migrate to form preplate, then subsequently generated neurons split the preplate to form the neocortical lamina—deeper layers first to upper layers last[1,2]. Spontaneous mutations in humans and mice have led to identification of several key genes essential to patterned neuronal migration in neocortex, and significant progress has been made in understanding how these genes direct brain development in general[3,4]. Currently, one of the least understood of these is *DCX*, an X-linked gene present only in vertebrates and expressed by migrating neurons[5–8]. Both the cellular expression pattern and a demonstrated role in microtubule stabilization has led to proposals that DCX protein is important for nuclear translocation and/or process elongation during radial migration[5,6,9–11]. Direct *in vivo* evidence for a specific cellular role of DCX has been difficult to obtain without a loss-of-function animal model that mimics the human neocortical phenotype[12]. A recently described mouse knockout of *Dcx* shows malformation of hippocampus, but shows no apparent malformation of neocortex[12]. In the present study, we applied RNAi technology combined with *in utero* electroporation to determine the role of DCX in radial migration during development of rat neocortex. In contrast to genetic knockout of *Dcx* in mice, we show that RNAi of DCX blocks radial migration in rat neocortex, and leads to a cortical phenotype similar to that observed in humans with *DCX* mutations.

RESULTS

In utero RNAi of DCX

Genetic compensation and/or species differences may account for the fact that a mouse knockout does not show an expected phenotype. Therefore, we developed a method of *in utero* RNAi to knock down DCX protein levels in migrating neocortical neurons in rats. Plasmids encoding short hairpin RNA[13] (**Fig. 1a**) along with plasmid encoding eGFP to mark transfected cells were co-transfected by *in utero* electroporation[14]. To first determine the effectiveness of *in utero* RNAi in developing rat brain, we transfected four different combinations of plasmids on embryonic day 14 (E14), dissociated cortical hemispheres one and four days after transfection, and processed dissociated cells for DCX immunocytochemistry (**Fig. 1b**). The percentage of transfected cells ($eGFP^+$) that were also immunopositive for DCX protein was determined by counting 100–300 $eGFP^+$ cells per embryo (4–5 embryos per transfection condition, $n = 35$). One day after transfection with eGFP plasmid alone, 33 ± 5.7% (mean ± standard error of the mean, s.e.m.) of GFP^+ cells were also DCX^+. Similarly, approximately 30% of GFP^+ cells were DCX^+ when transfected with either hairpin plasmids containing a region of DCX coding sequence (CDShp; 29.7 ± 2.3%) or with sequence matching the 3′UTR of DCX save for three point mutations (3UTRm3hp; 31 ± 3.9%). In contrast, only 5.7 ± 1.3% of GFP^+ cells were DCX^+ when transfected with the hairpin construct matching the 3′UTR of DCX (3UTRhp; **Fig. 1c**). These results show the effectiveness of 3UTRhp at decreasing DCX protein expression in neocortical cells *in vivo*.

Four days after *in utero* transfection, there was an increase in DCX expression in all transfection conditions, although 3UTRhp continued to suppress DCX expression. Cells transfected with eGFP plasmid alone increased to 80.6 ± 2.1% DCX^+, and those transfected with 3UTRm3hp increased to 70.3 ± 2.6% DCX^+. As cells are initially transfected at the ventricular zone (VZ) surface where DCX expression is the lowest, the increased signal over time is likely to reflect increased DCX expression as cells migrate out of the VZ. In addition to the general increase in DCX, a new difference appeared between transfection conditions. Specifically, cells transfected with CDShp were now significantly less positive for DCX (53.6 ± 7.6%) than cells transfected with either 3UTRm3hp or eGFP plasmid alone ($P < 0.001$, t-test). Four days after transfection, cells transfected with

Department of Physiology and Neurobiology, University of Connecticut, 3107 Horsebarn Hill Road, U-4156, Storrs, Connecticut 06269, USA. Correspondence should be addressed to J.L. (loturco@uconn.edu).

Published online 16 November 2003; doi:10.1038/nn1153

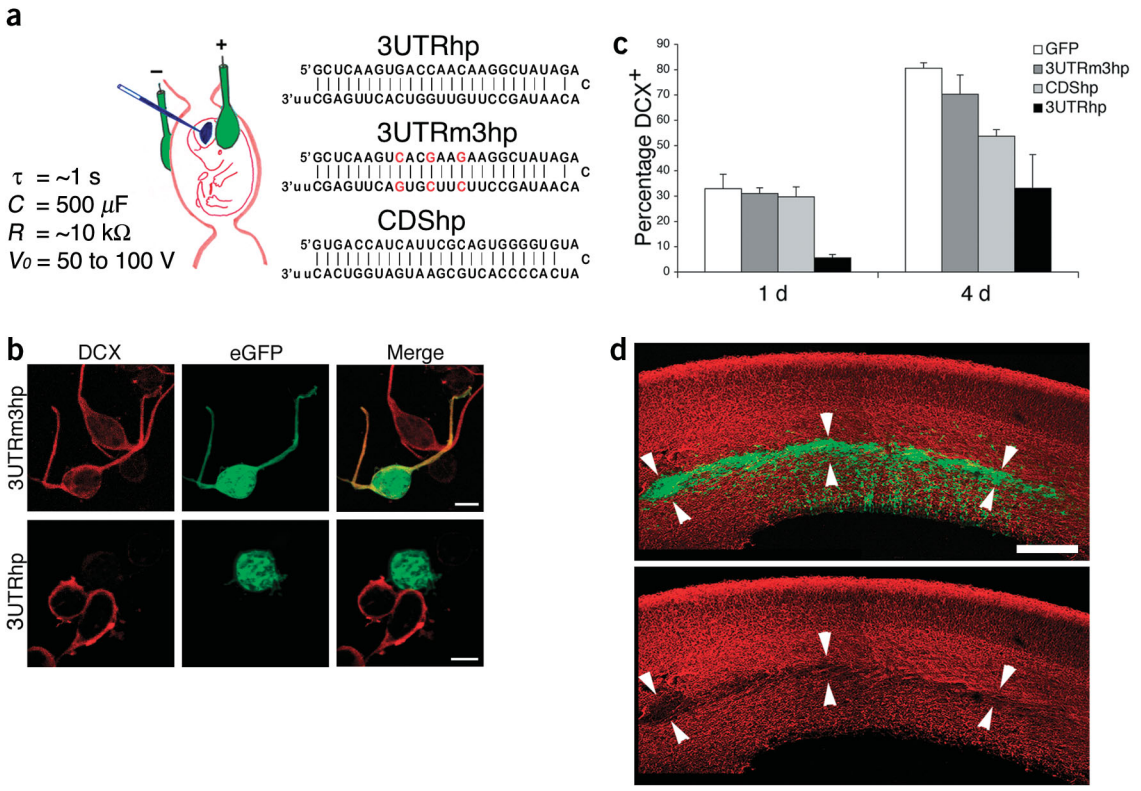

Figure 1 *In vivo* RNAi of DCX protein expression by *in utero* electroporation of plasmids encoding short hairpin RNA. (**a**) Schematic representation of *in utero* electroporation methods and the sequences of the hairpins used in this study: DCX 3′ untranslated region (3UTRhp), three point mutations (red) control sequence of DCX3UTR (3UTRm3hp) and DCX coding sequence (CDShp). (**b**) Representative confocal images of DCX protein expression (red) in dissociated cells assessed 4 d after *in utero* electroporation. An eGFP+3UTRm3hp-transfected cell is DCX^+ (top), whereas an eGFP+3UTRhp transfected cell is DCX^- (bottom). (**c**) Quantitative results for DCX expression in cell dissociation experiments, 1 and 4 d after electroporation of four different plasmid combinations (eGFP alone, eGFP+3UTRm3hp, eGFP+CDShp and eGFP+3UTRhp). 3UTRhp was most effective at decreasing DCX expression, and CDShp had a lesser but significant effect at 4 d after transfection. (**d**) Four days after E14 transfection of eGFP+3UTRhp, a band of $eGFP^+$ cells in the IZ is coextensive with a region of reduced DCX immunoreactivity, further indicating the effectiveness of RNAi of DCX (arrows; red). Scale bars: (**b**) 5 μm (**d**) 200 μm.

3UTRhp continued to show the lowest amount of DCX positivity (32.7 ± 13.3%) of the four transfection conditions. In addition to data from dissociated cells, sections prepared from 3UTRhp-transfected brains show gaps in DCX immunopositivity that are coextensive with aggregates of transfected (GFP^+) cells in the intermediate zone (IZ; **Fig. 1d**). Together, these results indicate that short hairpin RNA targeted against the 3′UTR of DCX effectively decreases DCX and does so, as previously demonstrated for RNAi, in a highly sequence-specific manner. Furthermore, the hairpin directed against a region of coding sequence in DCX also significantly decreases DCX expression, but more slowly and to a lesser extent. RNAi by *in utero* electroporation is therefore an effective means to decrease the levels of targeted proteins *in vivo*. In addition, this approach offers the advantages of spatial and temporal control, as well as variable effectiveness of different targeting constructs.

RNAi of DCX inhibits radial migration

To determine whether RNAi of DCX alters the normal migration of neocortical neurons in rat neocortex, we examined the positions of transfected cells 1 and 4 d after *in utero* transfection on E14. One day after electroporation, there was no obvious difference in the position of cells in the four different transfection conditions ($n = 23$; **Fig. 2**). At this time, cells are primarily within the ventricular zone (VZ) and lower regions of the IZ. Four days after transfection with eGFP alone ($n = 8$) or 3UTRm3hp ($n = 26$), all hemispheres examined had a majority of transfected neurons within the CP (54 ± 8.2% and 52 ± 7.2% of transfected cells), whereas hemispheres transfected with 3UTRhp ($n = 37$) had a small percentage of transfected cells within the CP (3.4 ± 1.9%; **Fig. 2**). In addition, a heterotopic aggregation of transfected cells formed within the IZ of all 3UTRhp transfected cortices (**Figs. 1d, 2, 3a**) but in none of the GFP- or 3UTRm3hp-transfected cortices. Hemispheres transfected with CDShp also showed a disruption in migration, although less severe than that observed with 3UTRhp: 18 ± 1.8% of transfected cells reached the CP in hemispheres transfected with CDShp ($n = 21$). Thus, the effectiveness of the two hairpin constructs directed against DCX in decreasing DCX expression correlated with the severity of the migration disruption. Such a correlation is further evidence of the specificity of RNAi in these experiments and shows that intermediate *in vivo* phenotypes, which may be useful in studying genetic interactions, can be generated with RNAi technology *in vivo*.

RNAi of DCX and morphology of migrating neurons

To determine the cellular function of DCX in migrating neocortical cells, we began by examining the morphology of cells that were co-transfected with 3UTRhp. As shown above, 4 d after transfection, GFP^+ neurons are largely confined to the IZ. These neurons within the IZ were either highly multipolar cells and located within the middle and lower portions of the IZ, or radially oriented bipolar cells within the upper regions of IZ just below the CP (**Fig. 3a**). The multi-

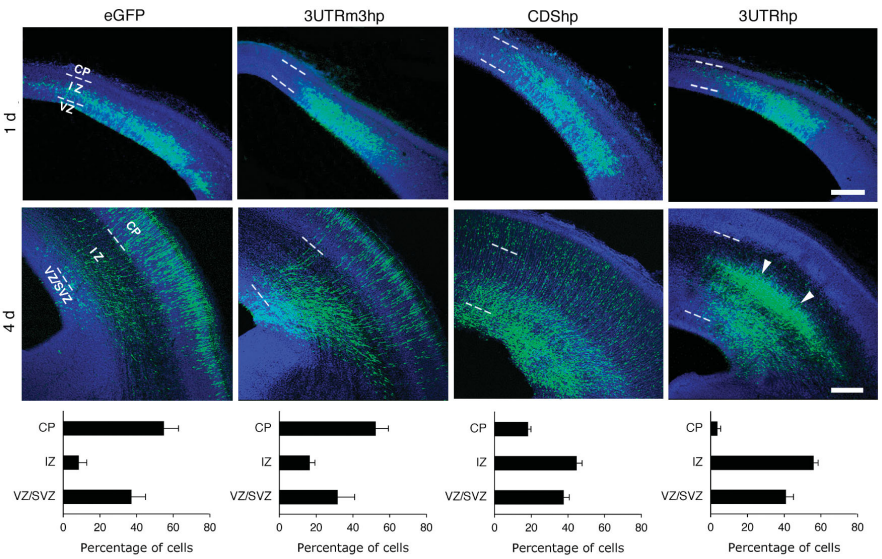

Figure 2 Disrupted radial migration by RNAi of DCX. Representative coronal sections of rat brains reveal migration of transfected cells 1 and 4 d after transfection on E14. One day after transfection, transfected cells in all four conditions are positioned similarly within the VZ and IZ, and no cells have yet reached the CP. Four days after transfection, a similar percentage of transfected cells have migrated into the CP of eGFP and eGFP+3UTRm3hp transfected hemispheres (54 ± 8.2% and 52 ± 7.2% of cells), whereas fewer (18 ± 1.8%) transfected cells have migrated to the CP in eGFP+CDSh-transfected hemispheres, and even fewer (3.4 ± 1.9%) in hemispheres transfected with eGFP+3UTRhp. All sections were counterstained with TO-PRO-3 (blue) nuclear counterstain, except for the 4-d CDShp section, which was stained with an antibody against nestin (blue). All scale bars: 200 μm.

polar cells in the IZ were TUJ1$^+$, indicating their neuronal identity, but lacked a clear leading or trailing process typical of radially migrating neurons (**Fig. 3b**). These cells were also DCX$^-$, indicating effective RNAi (**Fig. 3b**). In contrast, the bipolar radially oriented cells were both DCX$^+$ and TUJ1$^+$, and they had a leading radial process that in some cases extended into the CP (**Fig. 3c**). They were more prevalent in CDShp than in 3UTRhp transfected brains. These results, combined with the cell dissociation data showing an increase in DCX expression in 3UTRhp-transfected hemispheres, suggest that the radially oriented DCX$^+$ cells may not be directly affected by RNAi. This could indicate that they were delayed in migration by non–cell-autonomous effects from neighboring DCX$^-$ cells. Alternatively, the impaired radial migration of these bipolar DCX$^+$ cells may be a result of either an earlier decrease in DCX expression which then recovered or a continued decrease in DCX protein levels that is not detectable by non-quantitative immunocytochemistry.

Non-cell-autonomous component of disrupted radial migration

To determine whether the migration disruption created by DCX RNAi operates solely cell-autonomously or whether there is a non-cell-autonomous component as well, we developed a method of sequential *in utero* electroporation and performed BrdU labeling experiments. Unlike simultaneous co-transfections, sequential transfections label two differentially transfected cohorts of cells (**Fig. 4a**). To address the difference between sequential and simultaneous co-transfection *in vivo*, we show that when DsRed and eGFP plasmids are transfected simultaneously, most cells express both proteins (**Fig. 4a**). If, however, DsRed plasmid is transfected first, followed approximately 30 min later by eGFP plasmid, then most cells express only one or the other fluorescent protein (**Fig. 4a**). We found that 4 d after sequential transfection of control plasmids at E14 (DsRed then eGFP), separate red and green fluorescent populations of cells were distributed similarly throughout the IZ and CP (**Fig. 4b**; 4 of 4 brains). Note that the yellow in **Figure 4b** is largely due to the low magnification and not significant co-transfection of DsRed and eGFP (see **Fig. 4a** for higher magnification). In contrast, when DsRed and then eGFP+3UTRhp are sequentially transfected, red fluorescent cells reach the cortical plate only in regions where there are no or very few green fluorescent cells in the underlying IZ (5 of 6 brains). Many red fluorescent cells migrate into the upper regions of CP, but these are found only within regions of CP flanking the densest concentrations of green fluorescent cells in the IZ. In other words, the DsRed transfected cells appear unable to migrate through the

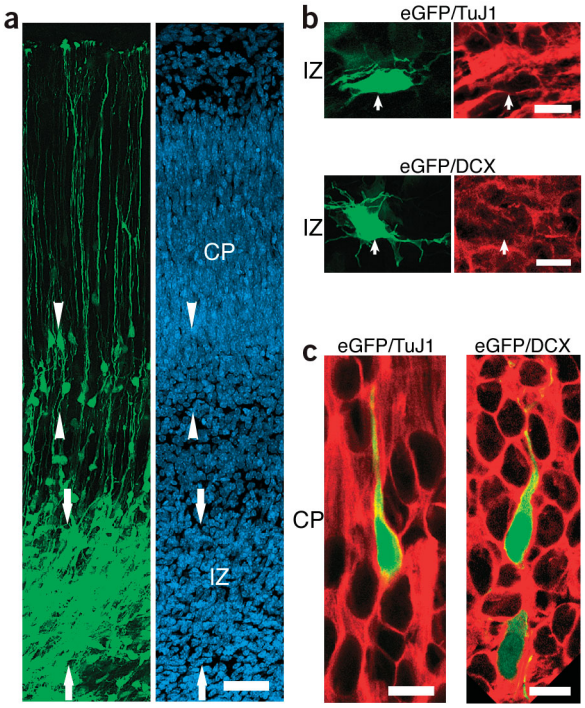

Figure 3 Morphology of neurons in hemispheres targeted with RNAi of DCX. (**a**) Four days after 3UTRhp transfection, most eGFP+ cells are stalled within the IZ (arrows), and a smaller group of eGFP$^+$ cells with bipolar morphologies are just below and within the lower CP (arrowheads). (**b**) Multipolar eGFP$^+$ cells are prevalent within the band of stalled cells in the IZ at 4 d after transfection with 3UTRhp. These cells are positive for the neuronal marker TuJ1 (red in top image), but are negative for expression of DCX (red; lower image). (**c**) Radially oriented cells located on the edge of the CP at 4 d after transfection with 3UTRhp are positive for both TuJ1 (left; red) and DCX (right; red). Scale bars: (**a**) 40 μm (**b**) 10 μm (**c**) 10 μm.

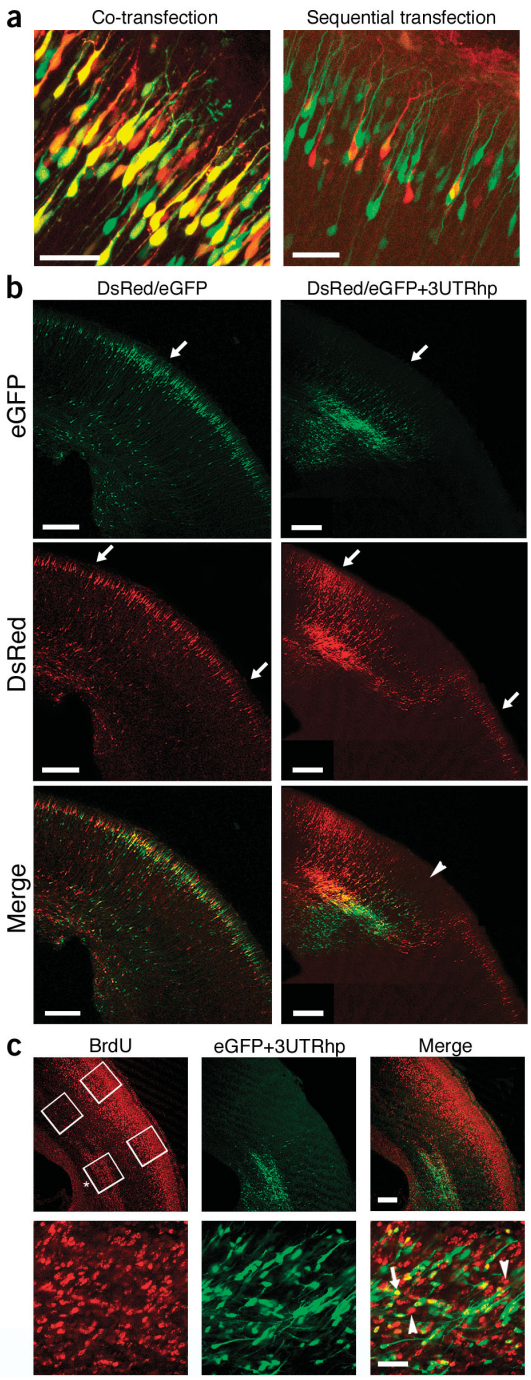

Figure 4 Non-cell-autonomous component of migration disruption by RNAi of DCX. (**a**) Co-transfection of plasmids encoding eGFP and DsRed results in 80% double-labeled cells (yellow) while sequential transfection labels largely non-overlapping cell populations (2% double-labeled cells). (**b**) Sequential electroporation of DsRed and then eGFP (left column) resulted in a similar distribution of eGFP$^+$ and DsRed$^+$ cells in the upper layers of the CP and IZ 4 d after transfection on E14. In contrast, sequential electroporation of DsRed and then eGFP+3UTRhp (right column) resulted in a lack of eGFP$^+$ cells in the upper CP (arrow, top panels) and a flanking distribution of DsRed$^+$ cells in the CP (arrows, middle panels). The gap in the distribution of DsRed$^+$ cells in the CP (arrowhead, bottom-right) above the band of eGFP cells in the IZ indicates a disruption in migration of DsRed$^+$ cells in the region of eGFP+3UTRhp transfection. (**c**) Aggregation of BrdU$^+$ cells within, but not outside of, regions of IZ with eGFP+3UTRhp transfection (squares indicate regions of CP and IZ with and without significant concentrations of BrdU$^+$ red cells). The aggregation of BrdU$^+$ cells in the IZ is coextensive with the transfected cells (eGFP and Merge). Enlarged view of the aggregation of BrdU$^+$ and eGFP$^+$ cells in the IZ indicate that many of the BrdU$^+$ cells are not transfected. Arrow indicates an example of a BrdU$^+$/eGFP$^+$ cell, and arrowheads indicate BrdU$^+$/eGFP$^-$ cells. Scale bars: (**a**) 40 μm (**b**) 200 μm (**c**) top, 100 μm; bottom, 20 μm.

cells in regions affected by RNAi, but can migrate into the CP in regions lacking cells affected by RNAi.

In addition to sequential electroporation experiments, we tested for a non-cell-autonomous component of RNAi of DCX. We used BrdU experiments. BrdU should label all VZ cells in S-phase of the cell cycle, whereas electroporation labels a relatively small subset of VZ cells. Therefore, if significant numbers of BrdU$^+$/eGFP$^-$ cells remain trapped within heterotopic arrangements of GFP$^+$ cells in the IZ 4 d after 3UTRhp transfection, then this would indicate a non-cell-autonomous influence of DCX RNAi. Four days after the E14 transfection and BrdU injections, only 4% of BrdU$^+$/eGFP$^-$ cells in the IZ and CP were still within the IZ, and 96% were within the CP in regions of cortex outside of transfection (**Fig. 4c**). In contrast, 22% of BrdU$^+$/eGFP$^-$ cells were within the IZ in regions of cortex transfected with 3UTRhp (n = 4 hemispheres), and the BrdU$^+$ cells formed heterotopic arrangements of cells in the IZ that were not apparent in regions outside of transfection in the same or opposite (not shown) hemisphere. In addition, BrdU$^+$/eGFP$^-$ and BrdU$^-$/eGFP$^-$ cells in the IZ heterotopias were DCX$^+$, and therefore they were not directly affected by RNAi. Together with the sequential electroporation data, we conclude that inhibiting DCX expression in a cohort of migrating neocortical neurons can disrupt radial migration of other migrating neurons within the IZ.

Subcortical band heterotopia

Human males carrying mutations in *DCX* typically have a severe global malformation of cortex, lissencephaly, whereas females heterozygous for *DCX* mutations typically develop double-cortex syndrome, or subcortical band heterotopia[15]. Heterotopia form within the white matter, most likely because of stalled migration within the IZ, and they are believed to form because X-inactivation in females results in somatic mosaicism[16]. The *in utero* electroporation method we used here also creates a mosaic of disrupted and undisrupted cells, so to determine the consequence of this mosaicism on the final form of neocortex, we allowed several animals to be born and mature to ages when all layers of neocortex have formed (postnatal days 14, 28 and 105). In all 12 postnatal brains examined, subcortical band heterotopias formed beneath normotopic cortex (**Fig. 5a**,**b**). These heterotopias were distinct and well-bounded by the subcortical white matter, and they did not mix with the overlying normotopic layers of neocortex. Consistent with the partially non–cell-autonomous nature of the disruption, cells within the heterotopia were both eGFP$^+$ and eGFP$^-$ (**Fig. 5c**).

To confirm that the induced heterotopias contain functional neurons, we made whole-cell electrophysiological recordings from cells within the heterotopia. All cells (n = 6) generated multiple action potentials (**Fig. 5d**), and some had morphologies similar to atypically oriented pyramidal neurons. In addition, local extracellular stimulation initiated synaptic responses in these neurons (**Fig. 5d**). The presence of such well-formed malformations containing functional neurons indicates that lack of DCX causes a failure of many neurons to integrate into normal layers of neocortex and to instead form a separate heterotopic structure containing physiologically functional neurons and synapses.

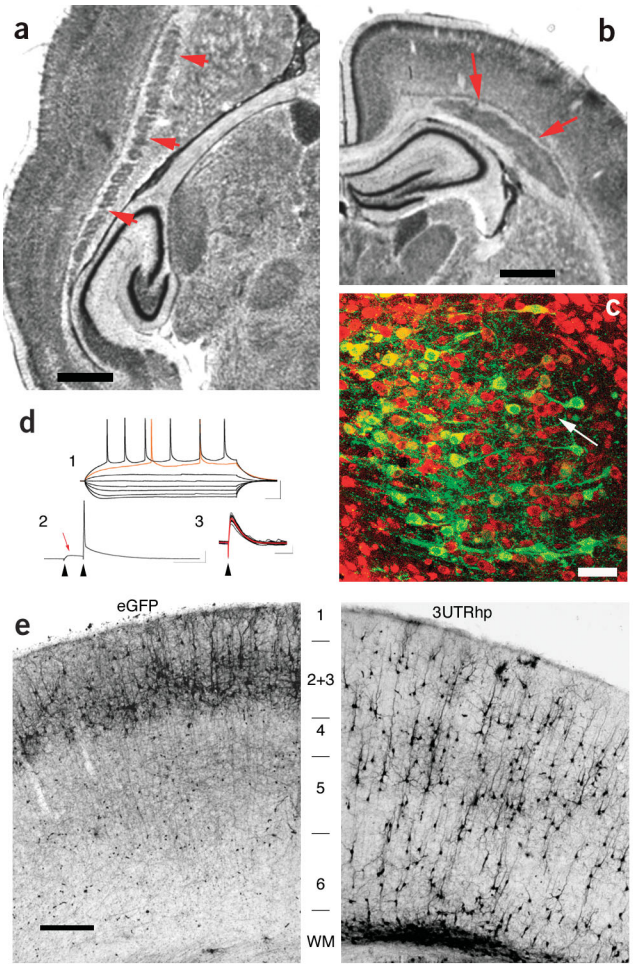

Figure 5 Creation of double cortex syndrome by RNAi of DCX. (**a**) Horizontal and (**b**) coronal sections of P14 rat brains show subcortical band heterotopia (arrows) after electroporation of eGFP+3UTRhp at E14. (**c**) Nissl counterstain (red) indicates that many neurons within the heterotopia do not express eGFP (arrows). (**d**) Whole-cell recordings of eGFP cells within the heterotopia show that these cells have neuronal physiologies. Cells show repetitive discharges upon intracellular current injection (1) and synaptic responses after local extracellular stimulation (2 and 3). (**e**) Immunostaining for eGFP in P14 rat brains revealed exclusive labeling of cortical layer 2+3 pyramidal neurons in control brains, whereas transfected neurons appeared scattered throughout all layers of 3UTRhp-transfected brains. Scale bars: (**a**) 1 mm (**b**) 1 mm (**c**) 50 μm (**d**1) 50 ms/20 mV (**d**2) 50 ms/15 mV (**d**3) 50 ms/2 mV (**e**) 250 μm.

Disrupted laminar placement

In all brains where heterotopia was induced by RNAi, there was always a well-formed region of normatopic cortex above the heterotopia into which eGFP$^+$ neurons had migrated. Therefore, some transfected cells in 3UTRhp-transfected brains can eventually enter the developing neocortical layers. In the mature cortex, the transfected neurons in normotopic cortex occupied abnormal laminar positions relative to cells in brains transfected with eGFP alone in neighboring embryos at the same developmental time. Transfected pyramidal neurons in brains transfected at E17 with eGFP alone came to occupy upper layers of neocortex, as is appropriate for neurons generated at that time (**Fig. 5e**). Pyramidal neurons in brains transfected with 3UTRhp+eGFP, however, were scattered across several neocortical lamina. These results indicate that loss of DCX expression can result not only in subcortical band heterotropias, but also in altered migration to neocortical lamina.

RNAi of DCX impairs radial migration in mouse neocortex

A recently described mouse *Dcx* knockout shows normal neuronal migration in neocortex[12]. Considering the difference between our current results in rats with those in the *Dcx* knockout mouse, we applied RNAi and *in utero* transfection methods to mice to determine whether the difference was due to species differences or a difference in the method of disruption. The region of 3′UTR targeted by 3UTRhp has the identical sequence in rat and mouse, so we transfected either 3UTRhp or the 3UTRm3hp construct that has three point mutations into E13 mouse embryos (**Fig. 1a**). We found similar results for both rodent species at 3 or 4 d after transfection ($n = 5$; **Fig. 6**). In mice, as in rats, RNAi of DCX by transfection of 3UTRhp led to failed migration to the cortical plate (8.5 ± 2.8% of transfected cells) and in an accumulation of cells in the IZ (62.5 ± 3.1% of transfected cells). In contrast, 54.7 ± 6% of transfected cells reached the CP, and 25.6 ± 3.7% of cells were within the IZ in hemispheres transfected with 3UTRm3hp (**Fig. 6**). Species differences, therefore, are not a likely reason for the difference between the knockout data and the RNAi data presented here, and there may be molecular compensatory responses engaged by genetic knockout but not by RNAi.

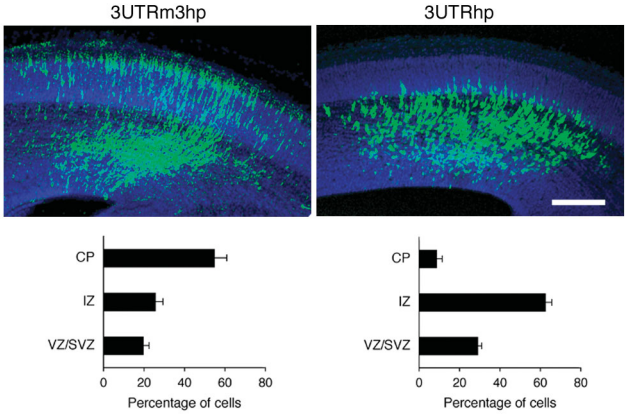

Figure 6 RNAi of DCX in mice disrupts radial migration in neocortex. Three days after transfection at E13 in mice, 54.7 ± 6% of eGFP$^+$ cells were in the CP of 3UTRm3hp-transfected hemispheres, whereas 8.5 ± 2.8% of eGFP$^+$ cells were within the CP of 3UTRhp-transfected hemispheres and 62.5 ± 3.1% were stalled within the IZ ($n = 5$). Scale bar, 200 μm.

DISCUSSION

Our experiments introduce an important addition to traditional mouse knockout studies for studying loss-of-function effects during brain development. Although the differences between the previously described DCX knockout phenotype and the phenotype described here using RNAi may at first seem paradoxical, there are several important differences between the two methods: (i) the time of disruption is temporally discrete in the RNAi approach and is determined largely by the transfection time (ii) only a subset of cells are targeted for disruption in otherwise normal tissue with RNAi and (iii) as it is unlikely that any RNAi is 100% effective, some amount of targeted protein and mRNA is present in cells targeted with RNAi. All three of these differences may contribute to the lack of a compensa-

tory response that may be otherwise activated in genetic knockouts. For example, early genetic deletion may allow cortical cells time to express genes that can compensate for loss of DCX. There are other possible compensatory actions: upregulation of extracellular migration guides in cortical tissue when every cell lacks DCX and/or small amounts of DCX mRNA or protein present within RNAi-treated cells may inhibit upregulation of other, as yet unidentified, genes that compensate for DCX. Future investigations into the possible compensatory mechanisms engaged by genetic deletion, but not by RNAi, could lead to identification of regulatory control mechanisms important to neuronal migration. Another advantage of the RNAi approach is that it can be used to model deficits in human brain development in species, such as the rat, in which knockout experiments are difficult.

Since blocking DCX expression with RNAi impairs all radial migration, it appears that our results are consistent with previous models proposing that DCX is important for both modes of radial migration[17] in developing neocortex[5,6,9–11]. Some disrupted neurons adopt an atypical morphology and extend exuberant multipolar processes within the IZ, suggesting impairment in growth of radial neurites, and other bipolar cells are impaired in reaching the top of the cortical plate, suggesting an impairment in nuclear translocation. More generally, DCX may be required for migrating cells to organize appropriate cytoskeletal responses to external signals that direct radial migration. Results from sequential transfection and BrdU experiments further suggest that disruption in DCX by RNAi interferes with radial migration both cell–autonomously and non–cell-autonomously. Such non–cell-autonomous inhibition may indicate a property of cooperative radial migration in neocortex similar to that present in other migrating populations of neurons[18]. The combination of non-cell-autonomous disruption and a potential role in both modes of radial migration may help to explain why different mutant DCX alleles lead to different malformation severities in humans[16,19].

The finding that DCX RNAi causes some neurons to occupy inappropriate laminar positions suggests that, in addition to subcortical band heterotopia, humans with mutations in DCX may have scattered ectopic neurons within normotopic cortex. We speculate that the altered laminar position may result from cells delayed in their normal migration either cell- or non–cell-autonomously. The two types of migration disruption— subcortical band heterotopia and atypical laminar position—may correspond to the two types of cells observed in the IZ 4 d after transfection with 3UTRhp. That is, the multipolar cells without a radial process may become the neurons within the heterotopia, and the radially oriented DCX$^+$ cells may come to occupy inappropriate lamina in normotopic cortex. Either of these developmental disruptions could have important functional implications for neocortex. Now that a loss-of-function animal model for DCX has been established, it should be possible in future studies to relate specific developmental alterations with functional changes associated with DCX mutations such as epilepsy and mental retardation.

METHODS

shRNA and *in utero* electroporation. Cells were transfected *in vivo* by *in utero* electroporation. Three different shRNA constructs based on the mU6pro vector[13] were used. First, we used doublecortin (*DCX*) 3′ untranslated region (DCX 3′UTR) hairpin siRNA sequence (5′-GCUCAAGUGACCAACAAGGCUAUAGACACAAUAGCCUUGUUGGUCACUUGAGC-3′; a blast search for short sequences returned matches to only two mRNA sequences in the data base: rat and mouse *Dcx*). Second, we used the DCX coding sequence (DCX CDS) hairpin siRNA sequence (5′-GUGACCAUCAUUCGCAGUGGGGUGUACAUCACCCCACUGCGAAUGAUGGUCAC-3′). Third, we used the DCX 3′UTR mutation hairpin siRNA sequence (5′-GCUCAAGUCACGAAGAAGGCUAUAGACACAAUAGCCUUCUUCGUGACUUGAGC-3′). To fluorescently label transfected cells, the plasmids CA-gap-eGFP (gift from A. Okada and S.K. McConnell[20]) and CA-DsRed (gift from A. Nishiyama, University of Connecticut, Storrs) were used. Plasmids were transfected by *in utero* electroporation. Briefly, multiparous Wistar rats, 14–17 d gestation, were anesthetized with Ketamine/Xylazine (100/10 mixture, 0.1 mg per g body weight, intraperitoneally (i.p.)), the uterine horns exposed, and plasmids 1–3 μl with Fast Green (2 mg/ml; Sigma) were microinjected by pressure (General Valve picospritzer) through the uterus into the lateral ventricles of embryos by pulled glass capillaries (Drummond Scientific; 0.5 μg/μl for pLZRS-CA-gapEGFP and pCAGGS-DsRed, 1.5 μg/μl for shRNA constructs). Electroporation was accomplished by discharging a 500-μF capacitor charged to 50–100 V with a sequencing power supply. The voltage pulse was discharged across a pair of copper alloy oval plates (1 × 0.5 cm) pinching the head of each embryo through the uterus. For sequential electroporation, DsRed plasmid was injected first, then electroporated; 15–30 min later, a second injection of eGFP +/– shRNA plasmid(s) was made and electroporated. Animal protocols were approved by the University of Connecticut IACUC.

Immunocytochemistry, confocal microscopy and electrophysiology. Cells in fetal and postnatal brain were phenotyped by immmunochytochemistry and electrophysiology. Fetal brains were removed and fixed in 4% paraformaldeyhde/PBS, and postnatal brains were removed and fixed in 4% paraformaldehyde/PBS after transcardial perfusion. Both fetal and postnatal brains were sectioned at 50–100 μm on a vibratome (Leica VT1000S) and processed for immunocytochemistry as free-floating sections. For acutely dissociated cell preparations, hemispheres were dissected and cells were dissociated and processed as previously described[21]. All cell counting for determining DCX positivity of eGFP$^+$ cells was determined without the experimenter knowing the identity of the transfection condition. Primary antibodies included mouse anti-nestin (1:100, Chemicon), goat anti-doublecortin (1:100, Santa Cruz) and rabbit anti-GFP (1:300, Chemicon). Fluorescently conjugated secondary antibodies (Alexa 488, 568 or 633 from Molecular Probes or Cy-5 from Jackson) and biotin-conjugated secondaries were used for fluorescent or chromagen detection. In some tissue, nuclei were labeled with TO-PRO-3 (Molecular Probes) or counterstained with Neurotrace Nissl 530/615 (Molecular Probes). Images were acquired on either a Leica TCS SP2 confocal system (0.5–1.0 μm optical sections) or a Nikon Eclipse 400 with a Spot camera. Images were processed using Volocity LE (Improvision) and/or Adobe Photoshop 7. Methods for whole-cell recording, extracellular stimulation and biocytin reconstruction of neurons are similar to those previously described[22].

ACKNOWLEDGMENTS

R.L.R. and J.B.A. contributed equally to this work. We thank S. Korn, A. Moiseff and M. Paramasivam for helpful discussions and comments on drafts of the manuscript. We also thank D. Turner for the mU6pro vector. This work was supported by the National Institute of Mental Health (MH056524 to J.J.L.) and the National Institute of Child Health and Human Development (HD20806).

COMPETING INTERESTS STATEMENT

The authors declare that they have no competing financial interests.

Received 27 August; accepted 21 October 2003
Published online at http://www.nature.com/natureneuroscience/

1. Sidman, R.L. & Rakic, P. Neuronal migration, with special reference to developing human brain: a review. *Brain Res.* **62**, 1–35 (1973).
2. Marin-Padilla, M. The development of the human cerebral cortex. A cytoarchitectonic theory. *Rev. Neurol.* **29**, 208–216 (1999).
3. Gupta, A., Tsai, L.H. & Wynshaw-Boris, A. Life is a journey: a genetic look at neocortical development. *Nat. Rev. Genet.* **3**, 342–355 (2002).
4. Walsh, C.A. & Goffinet, A.M. Potential mechanisms of mutations that affect neuronal migration in man and mouse. *Curr. Opin. Genet. Dev.* **10**, 270–274 (2000).
5. Gleeson, J.G., Lin, P.T., Flanagan, L.A. & Walsh, C.A. Doublecortin is a microtubule-associated protein and is expressed widely by migrating neurons. *Neuron* **23**, 257–271 (1999).
6. Francis, F. *et al.* Doublecortin is a developmentally regulated, microtubule-associated protein expressed in migrating and differentiating neurons. *Neuron* **23**, 247–256 (1999).
7. des Portes, V. *et al.* A novel CNS gene required for neuronal migration and involved

in X-linked subcortical laminar heterotopia and lissencephaly syndrome. *Cell* **92**, 51–61 (1998).
8. Gleeson, J.G. *et al.* Doublecortin, a brain-specific gene mutated in human X-linked lissencephaly and double cortex syndrome, encodes a putative signaling protein. *Cell* **92**, 63–72 (1998).
9. Kato, M. & Dobyns, W.B. Lissencephaly and the molecular basis of neuronal migration. *Hum. Mol. Genet.* **12**, R89–96 (2003).
10. Feng, Y. & Walsh, C.A. Protein-protein interactions, cytoskeletal regulation and neuronal migration. *Nat. Rev. Neurosci.* **2**, 408–416 (2001).
11. Horesh, D. *et al.* Doublecortin, a stabilizer of microtubules. *Hum. Mol. Genet.* **8**, 1599–1610 (1999).
12. Corbo, J.C. *et al.* Doublecortin is required in mice for lamination of the hippocampus but not the neocortex. *J. Neurosci.* **22**, 7548–7557 (2002).
13. Yu, J.Y., DeRuiter, S.L. & Turner, D.L. RNA interference by expression of short-interfering RNAs and hairpin RNAs in mammalian cells. *Proc. Natl. Acad. Sci. USA* **99**, 6047–6052 (2002).
14. Takahashi, M., Sato, K., Nomura, T. & Osumi, N. Manipulating gene expressions by electroporation in the developing brain of mammalian embryos. *Differentiation* **70**, 155–162 (2002).
15. Gleeson, J.G. *et al.* Characterization of mutations in the gene doublecortin in patients with double cortex syndrome. *Ann. Neurol.* **45**, 146–153 (1999).
16. Gleeson, J.G. *et al.* Somatic and germline mosaic mutations in the doublecortin gene are associated with variable phenotypes. *Am. J. Hum. Genet.* **67**, 574–581 (2000).
17. Nadarajah, B., Brunstrom, J.E., Grutzendler, J., Wong, R.O. & Pearlman, A.L. Two modes of radial migration in early development of the cerebral cortex. *Nat. Neurosci.* **4**, 143–150 (2001).
18. Lois, C., Garcia-Verdugo, J.M. & Alvarez-Buylla, A. Chain migration of neuronal precursors. *Science* **271**, 978–981 (1996).
19. Gleeson, J.G. *et al.* Genetic and neuroradiological heterogeneity of double cortex syndrome. *Ann. Neurol.* **47**, 265–269 (2000).
20. Okada, A., Lansford, R., Weimann, J.M., Fraser, S.E. & McConnell, S.K. Imaging cells in the developing nervous system with retrovirus expressing modified green fluorescent protein. *Exp. Neurol.* **156**, 394–406 (1999).
21. Bittman, K.S. & LoTurco, J.J. Differential regulation of connexin 26 and 43 in murine neocortical precursors. *Cereb. Cortex* **9**, 188–195 (1999).
22. Gabel, L.A. & LoTurco, J.J. Electrophysiological and morphological characterization of neurons within neocortical ectopias. *J. Neurophysiol.* **85**, 495–505 (2001).